ISSN 1063-7834, Physics of the Solid State, 2011, Vol. 53, No. 4, pp. 834–839. © Pleiades Publishing, Ltd., 2011.
Original Russian Text © M.S. Molokeev, S.V. Misyul', V.D. Fokina, A.G. Kocharova, K.S. Aleksandrov, 2011, published in Fizika Tverdogo Tela, 2011, Vol. 53, No. 4, pp. 778–783.

PHASE TRANSITIONS

Structure Transformations during Phase Transitions in the $K_3WO_3F_3$ Oxyfluoride

M. S. Molokeev[a, *], S. V. Misyul'[b, **], V. D. Fokina[a], A. G. Kocharova[a], and K. S. Aleksandrov[a, b, †]

[a] *Kirensky Institute of Physics, Siberian Branch, Russian Academy of Sciences, Akademgorodok, Krasnoyarsk, 660036 Russia*
* *e-mail: msmolokeev@mail.ru*
[b] *Siberian Federal University, Svobodnyi pr. 79, Krasnoyarsk, 660041 Russia*
** *e-mail: misjul@akadem.ru*

Received August 11, 2010

Abstract—The structures of three phases of the $K_3WO_3F_3$ crystal have been determined from X-ray diffraction data obtained for a powder sample. The profile and structural parameters have been refined according to the technique implemented in the DDM program. The results obtained have been discussed using the group-theoretical analysis of the complete order parameter condensate, which takes into account the critical and noncritical atomic displacements and allows the interpretation of the experimental data. The sequence of structural transformations is found to be as follows: $Fm\bar{3}m \xrightarrow[(\eta_1, 0, 0)]{11-10(\Gamma_4^-)} I4mm \xrightarrow[(\eta_1, \eta_2, 0)]{11-10(\Gamma_4^-)} Cm$.

DOI: 10.1134/S1063783411040251

1. INTRODUCTION

The main structural elements in compounds of the general formula $A_2BMO_xF_{6-x}$ (A, B: K, Rb, Cs; M: Ti, Mo, W; $x = 1, 2, 3$) are noncentrosymmetric MO_xF_{6-x} oxyfluoride anions which, under specific conditions, allow the formation of polar structures with ferroelectric properties [1]. However, the majority of fluorine–oxygen compounds crystallize in the nonpolar phase of the cubic elpasolite-like structure with the face-centered lattice (space group $Fm\bar{3}m$, $Z = 4$) [1, 2], which, most likely, indicates a fluorine–oxygen disorder in the MO_xF_{6-x} anions. In the case when the A and B cations are equivalent, the compound has a cryolite structure (Na_3AlF_6). As the temperature decreases, the majority of the oxyfluorides undergo phase transitions of the ferroelastic or ferroelectric nature due to the ordering and small atomic displacements [1, 2]. Recently, there have appeared a number of publications devoted to more detailed investigations of the $Na_3MoO_3F_3$ [3] and $Tl_3MoO_3F_3$ [4] phases distorted at room temperature. It has turned out that the univalent cation size substantially affects the symmetry of the low-temperature ferroelectric phase: sodium cryolite has space group $P1$, while tallium cryolite has space group Pc.

A number of compounds of the general formula $A_2BMO_3F_3$ (A, B: K, Rb, Cs; M: W, Mo), including $K_3WO_3F_3$, were studied in [2, 5]. It was concluded that these compounds undergo two phase transitions $G_0 \longrightarrow G_1 \longrightarrow G_2$: during the first high-temperature phase transition, the cubic structure of the compounds transforms into the hexagonal noncentrosymmetric structure with the unit cell parameters $a_{hex} = a_{cub}/\sqrt{2}$ and $c_{hex} = \sqrt{3}\,a_{cub}$. A further decrease in temperature brings about one more phase transition, after which the point group of symmetry becomes trigonal or even triclinic.

The phase transitions in one of the representatives of the aforementioned series of compounds, namely, in the $K_3WO_3F_3$ cryolite, were studied earlier by the calorimetric methods [2, 6, 7]. Two structural transformations were found at the temperatures $T_1 = 452$ K and $T_2 = 414$ K with the following changes in the entropy: $\Delta S_1 = R\ln(1.68)$ and $\Delta S_2 = R\ln(1.42)$ [2, 6]. As was shown in [2], at temperatures higher than $T_1 = 452$ K, the $K_3WO_3F_3$ crystal has cubic symmetry (space group $Fm\bar{3}m$, $Z = 4$). Later, in [8], the parameters of the tetragonal crystal unit cell of the $K_3WO_3F_3$ compound at room temperature were determined to be $a = 30.70 \pm 0.02$ Å and $c = 43.70 \pm 0.03$ Å.

Our relatively recent comprehensive studies of this compound [6, 7, 9] showed that the distorted phase at room temperature has monoclinic symmetry (space group Cm) with the parameters of the base-centered monoclinic unit cell $a = 8.7350(3)$ Å, $b = 8.6808(5)$ Å, $c = 6.1581(3)$ Å, and $\beta = 135.124(3)°$; in the temperature range T_1–T_2, the intermediate phase cannot have the hexagonal unit cell.

Such significant discrepancies in the experimental data obtained by different authors require additional

† Deceased.

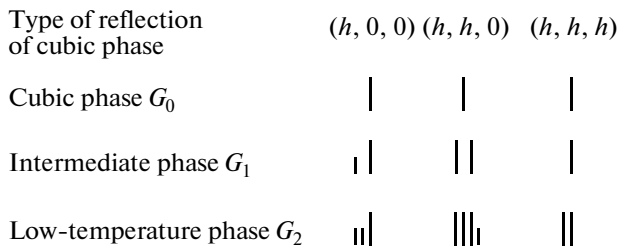

Fig. 1. Splitting of the main reflections of the cubic phase in $K_3WO_3F_3$ during phase transitions.

more careful structural studies of the $K_3WO_3F_3$ oxyfluoride. Moreover, all the preceding results, including the obtained changes in the entropy, do not answer the question as to what atoms or group of atoms, their displacements or orderings, are responsible for the phase transitions.

In order to elucidate the mechanism of transformations occurring in the $K_3WO_3F_3$ crystal, we performed the temperature X-ray powder diffraction studies of its structural characteristics and their changes during the phase transitions.

2. SAMPLE PREPARATION AND EXPERIMENTAL TECHNIQUE

In order to synthesize the $K_3WO_3F_3$ compound, we used potassium tungstate, potassium fluoride, and hydrofluoric acid. The concentrated aqueous solution of potassium tungstate was slowly, with continuous mixing, added in a solution of potassium fluoride in hydrofluoric acid. During this process, the active chemical reaction $K_2WO_4 + 2KF + HF \longrightarrow K_3WO_3F_3 + KOH$ occurs with the solution heating. The white sediment precipitated as a result of the reaction was the powder of the $K_3WO_3F_3$ crystal which was used in our X-ray diffraction studies.

The X-ray diffraction patterns from the polycrystalline $K_3WO_3F_3$ samples were measured using an Anton Paar TTK450 temperature chamber installed on a D8-ADVANCE X-ray diffractometer (CuK_α radiation, θ–2θ scanning, VANTEC linear detector). Liquid nitrogen was used as a coolant. The scan step in angle 2θ was 0.016°; the exposition was 0.3 s in each point. The experiments were performed in the temperature range from 303 to 473 K with a step of 10 K, which allowed us to state the regularities in the change in the structural characteristics of the crystal during the phase transitions. To more reliably refine the structures of the initial and distorted phases in three temperature points (298, 433, and 513 K) disposed quite far from the phase transition temperatures, the exposition at each experimental step was increased to 0.9 s. The temperatures at which the experiments were performed excluded the influence of the transition phenomena.

3. EXPERIMENTAL RESULTS

The splittings of the X-ray reflections of the initial cubic phase observed in the X-ray powder diffraction patterns as temperature decreased (Fig. 1) show that the G_1 phase cannot have trigonal symmetry, as was assumed in [2], even after the first phase transition at $T_1 = 452$ K, and, in this case, the tetragonal system is most likely realized (Figs. 1 and 2). An analysis of the changes in the dominant reflection profiles during the transition ($T_2 = 414$ K) in the G_2 phase (Figs. 1 and 2) indicates an additional splitting of the reflections of (*h*, 0, 0) and (*h*, *h*, *h*) types. Here and in what follows, the indices of all the reflections are given with respect to the unit cell parameters of the cubic G_0 phase. Using the homology method [10], the reflection splitting in the X-ray diffraction patterns can be interpreted by the most probable sequence of the phase symmetries: cubic $\longrightarrow$ tetragonal $\longrightarrow$ monoclinic with the twofold axis along the preceded fourfold axis or the triclinic symmetry. Moreover, we take into account that both distorted phases are noncentrosymmetric [2].

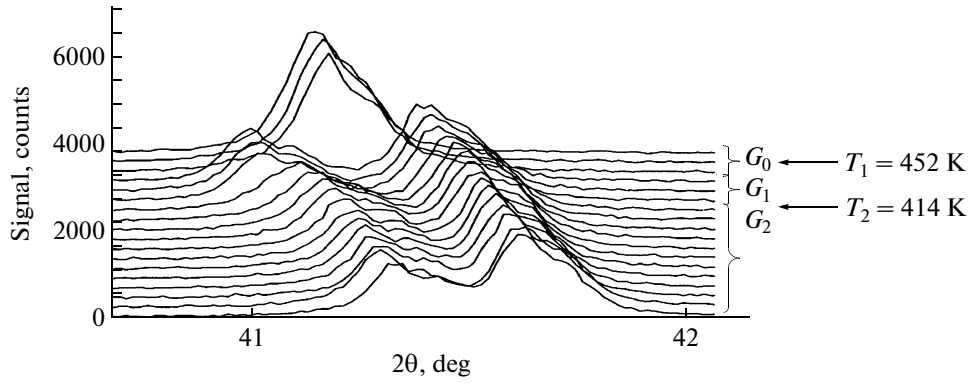

Fig. 2. Fragments of the X-ray diffraction patterns of the $K_3WO_3F_3$ compound with the (4, 0, 0) reflection at temperatures varying from 303 to 473 K in steps of 10 K.

Table 1. Parameters of the data acquisition and refinement of the structure

Parameter	$T = 298$ K	$T = 433$ K	$T = 513$ K
Space group	Cm	$I4mm$	$Fm\bar{3}m$
a_i, Å	a_0, 8.7350(3)	$1/2(a_0 - b_0)$, 6.1676(1)	a_0, 8.7958(1)
b_i, Å	b_0, 8.6901(4)	$1/2(a_0 + b_0)$, 6.1676(1)	b_0, 8.7958(1)
c_i, Å	$(c_0 - a_0)/2$, 6.1569(3)	c_0, 8.7997(2)	c_0, 8.7958(1)
β, deg	135.168(3)	90	90
V, Å^3	329.52(3)	334.74(1)	680.48(2)
Z	2	2	4
2θ angle range, deg	5–100	5–100	5–100
Number of reflections	360	81	37
Number of parameters refined	19	16	7
R_B, %	3.93	3.96	1.83
R_{DDM}, %	15.27	14.99	12.20
Order parameter η	$(\eta_1, \eta_2, 0)$	$(\eta_1, 0, 0)$	(0, 0, 0)
Experimental entropies	$R\ln 1.42$	$R\ln 1.68$	–
Calculated entropies	$R\ln 2$	$R\ln 2$	–

Note: R_B is the Bragg integral discrepancy factor; R_{DDM} is the profile discrepancy factor determined with the DDM program.

Table 2. Atomic coordinates, isotropic thermal parameters B_{ISO}, and position occupancies p in the $K_3WO_3F_3$ structure

Atom	p	X	Y	Z	B_{ISO}, Å^2
$T = 513$ K, $Fm\bar{3}m$					
W	1.0	0	0	0	3.90(4)
K1	1.0	1/2	1/2	1/2	6.9(1)
K2	1.0	1/4	1/4	1/4	5.8(1)
F	0.5	0.219(2)	0	0	4.3(3)
O	0.03125	0.192(3)	0.092(2)	0	4.4(7)
$T = 433$ K, $I4mm$					
W	1.0	1/2	1/2	1/2	3.82(4)
K1	1.0	0	0	0.497(8)	9.5(3)
K2	1.0	1/2	0	0.262(2)	5.2(2)
F1	0.5	0.277(3)	0.277(3)	0.526(4)	4.1(6)
F2	1	0	0	0.217(2)	1.0(4)
O1	0.25	0.228(5)	0.606(5)	0.560(4)	4.1(6)
O2	0.25	0.110(6)	0.110(6)	0.822(5)	3(1)
$T = 293$ K, Cm					
W	1.0	0	0	0	4.5(1)
K1	1.0	–0.06(1)	0	–0.078(8)	7.1(9)
K2	1.0	0.006(3)	0.719(2)	0.470(5)	1.9(4)
F1	1.0	0.275(7)	0	0.07(1)	2.0(1)
F2	1.0	0.73(1)	1/2	0.46(1)	2.0(1)
F3	0.5	0.04(1)	0.204(7)	0.14(1)	2.0(1)
O1	1.0	0.80(1)	0	0.60(1)	2.0(1)
O2	1.0	0.81(1)	0	0.00(1)	2.0(1)

Further consideration of the experimental data will be based on the group-theoretical studies of the structural phase transitions in the crystals with space group $Fm\bar{3}m$ [11] and with the ISOTROPY [12] and ISODISPLACE [13] program packages. According to [10–12], the changes in the symmetry, which are indicated by the splittings of reflections, their extinctions, and the data on the ferroelectric character of the transitions [2], i.e., the absence of the inversion center, can be explained by the fact that, during the transition from the cubic phase, there appears a phenomenological order parameter, which is transformed according to the irreversible representation Γ_4^- (11–10) of space group $Fm\bar{3}m$ with the wave vector of the Brillouin zone center (point Γ, $k_{11} = 0$). These order parameters, which specify the symmetry of the distorted phase, are referred to as the critical parameters according to [14]. The structural distortions, atomic displacements and orderings related to the critical order parameters are also called critical. All denotations concerning the irreversible representations and the Brillouin zone points are given according to [15].

Table 1 presents the relations between the components of the phenomenological order parameter, the data on the symmetry of phases in $K_3WO_3F_3$, and relations between main translations of the unit cells of the initial cubic and distorted phases.

The structural models of the distorted phases were determined by traditional Patterson function method and also by the method in which the symmetry analysis of the initial structure is used [16]. The symmetry analysis of the cubic phase structure includes an anal-

ysis of the mechanical and permutational representations, and it allows the assumption of possible displacements and orderings of ions in the distorted phases based on knowing critical order parameters and critical irreversible representations. The critical displacements and the probability of occupying one or other positions by an atom in the unit cell are determined during refining the crystal structure. This possibility is implemented in the BRUKER-AXS TOPAS 4 program [16].

The profile and structural parameters were refined using a new procedure realized in the DDM program which has not yet widely used now [17].

The temperature dependences of the cubic unit cell parameters found during fitting the profiles by the DDM program are depicted in Fig. 3. As was noted above, the atomic coordinates, the occupancies of their positions, and the thermal parameters were refined using the data measured at temperatures of 298, 433, and 513 K. The peak shape was described by the Pearson VII function. The refined data on the structures of all phases of $K_3WO_3F_3$ are given in Tables 1 and 2, and the main bond lengths are listed in Table 3. The G_2 phase structure in $K_3WO_3F_3$ was even reported earlier [9]; however, despite the low discrepancy R factor (2.47%), the bond lengths d(W–O) were very short (1.48–1.63 Å), which casts a doubt upon the validity of the model. In this work, we proposed the model of the G_2-phase structure, which differs from the model described in [9] predominantly in the arrangement of the O atoms. The refinement of this model led to more realistic values of the bond lengths d(W–O) in the range 1.70–1.74 Å.

In the high-temperature G_0 phase at 513 K, the $K_3WO_3F_3$ crystal has a cubic cryolite structure. The primitive cell contains one W atom, two independent K atoms; and F atom occupies the 24*e* position with the occupation multiplicity of the position of 0.5. In the initial model, the O atom also occupies the 24*e* position with the same position occupation multiplicity of 0.5, and it was refined with an anisotropic thermal parameter. In this approximation, the discrepancy factor $R_B = 3.5\%$. As the O atom was placed to position 96*j* with the position occupation multiplicity of 3/96 and its position was further refined in the isotropic approximation, the discrepancy factor sharply decreased to $R_B = 1.83\%$. Similar disordering is also demonstrated by the arrangement of the O and F atoms in the monoclinic G_2 phase structure. Since the WO_3F_3 polyhedron in the monoclinic phase is distorted, and the O–W–O angles are not all close to 90° (Table 3), which is also confirmed by the data from [9], we, adding the elements of the cubic phase symmetry absent in the G_2 phase, obtain the disordering of the O and F atoms similar to that described above.

In the tetragonal G_1 phase at 433 K, the primitive cell of the $K_3WO_3F_3$ crystal contains one W atom, two independent K atoms, two independent F atoms, and two independent O atoms. The refinement of the model was stable. The choice of and the search for the structure of the low-temperature monoclinic phase at 293 K were performed in the same way as the search for the phase structure at 433 K. The refinement of the structure was also stable with a low discrepancy factor.

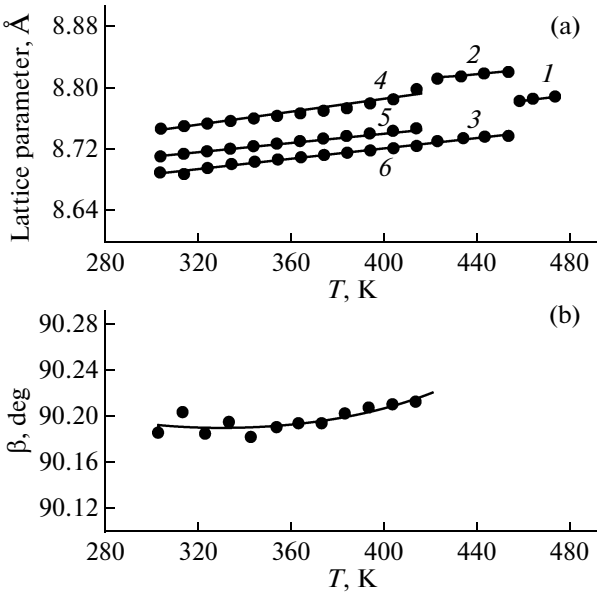

Fig. 3. Temperature dependences of (a) the unit cell parameters of (*1*) the cubic G_0 phase a_0, (*2*, *3*) tetragonal G_1 phase (*2*) c_1 and (*3*) $a_1\sqrt{2}$, and (*4*–*6*) monoclinic G_2 phase (4) a2, (*5*) $c_2\sqrt{2}$, and (*6*) b_2; and (b) the monoclinicity angle in the G_2 phase ($\beta - 45°$) of the $K_3WO_3F_3$ compound.

4. DISCUSSION OF THE RESULTS

In order to understand the mechanism of the phase transitions and the separation of leading (critical) atoms, we shall simulate the ordering of the WO_3F_3 octahedron with symmetry 3*mm* (C_{3v}) [18, 19]. Since the d(W–O) and d(W–F) distances are different, the WO_3F_3 octahedron can be represented as a vector directed from the center of the triangle built on the F atoms to the center of the triangle built on the O atoms. In the cubic unit cell, the WO_3F_3 octahedron is oriented so that this vector has the coordinates (x, x, x), where x is an arbitrary constant. Replacing the octahedron by the vector, it is easy to obtain the number of different orientations of WO_3F_3 in the cubic phase. Since the (x, x, x) position in the cubic phase has the multiplicity of 32, the number of the orientations of WO_3F_3 in a site is $N_0 = 32/Z = 32/4 = 8$, where $Z = 4$ is the number of the formula units in the cubic face-centered unit cell. Thus, there are eight different orientations of the WO_3F_3 octahedron in the cubic phase.

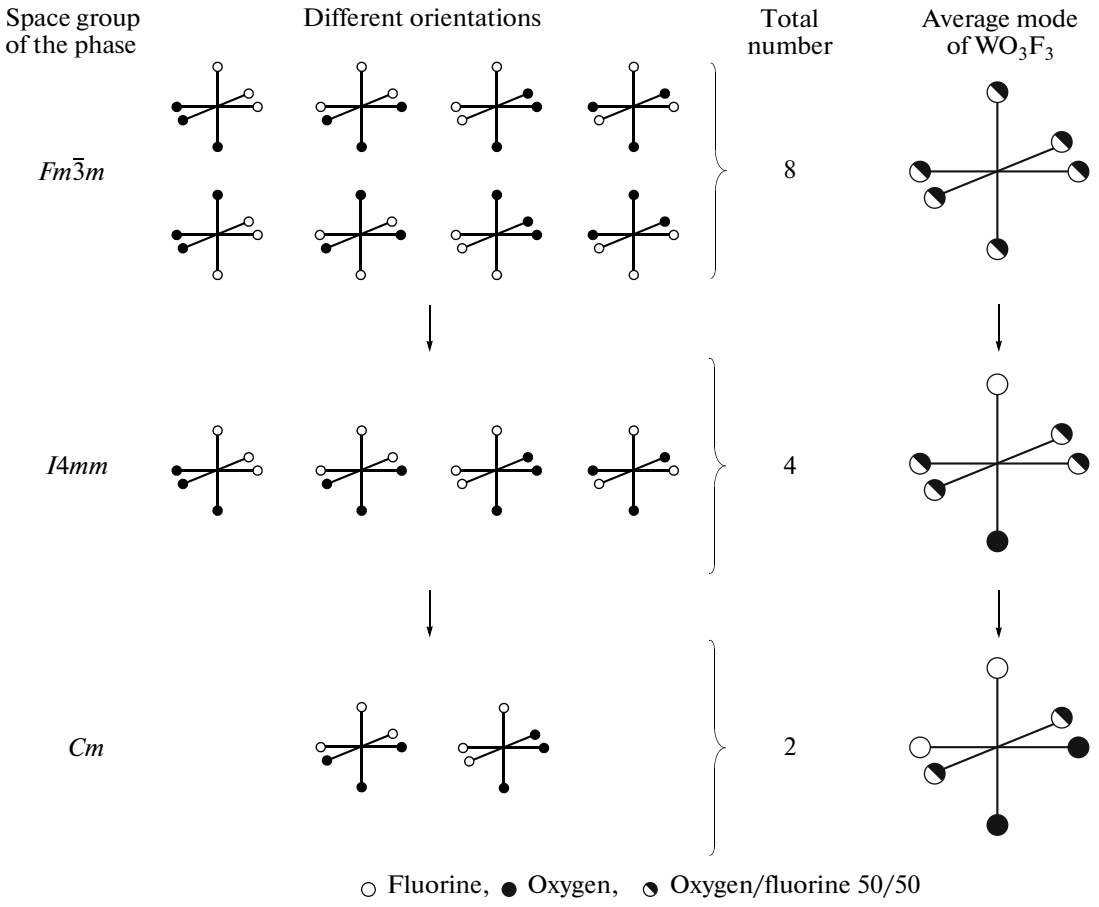

Fig. 4. Model of ordering in WO_3F_3.

Using the group-theoretical analysis of the permutation representation, we can determine which of these eight positions disappear and which of them are retained. Thus, we can state which of the octahedron orientations are retained after the phase transition if we know the critical order parameter transformed by a critical irreversible representation of the initial group. For this purpose, the ISODISPLACE program [13] is most suitable, since it not only operates with all space groups and representations, but also it visualizes the result. Finding the number of the retained orientations N_1, we can easily calculate the entropy change during the phase transition related to ordering of an atomic group ($\Delta S = R\ln(N_0/N_1)$).

As was noted above, the change in the symmetry during the phase transitions in $K_3WO_3F_3$ is caused by the critical three-component order parameter which is transformed by the Γ_4^- (11–10) representation.

During the phase transition $Fm\bar{3}m \longrightarrow I4mm$ at $T_1 = 452$ K, only one of three components of the order parameter has a nonzero value: (η_1, 0, 0) (Table 1). An analysis of the tetragonal G_1 phase structure shows that several of the O and F atoms are ordered during the phase transition. Moreover, the ordering is accompanied by a displacement of the K atoms with respect to their positions in the cubic lattice: Δr(K1) = (0, 0, –0.02) Å and Δr(K2) = (0, 0, 0.11) Å (here and in what follows, the components of all atomic displacements are given relative to the pseudo-cubic lattice). It is precisely the enumerated orderings and displacements of the atoms that are critical and, and they are transformed by the Γ_4^- (11–10) representation with the order parameter (η_1, 0, 0). Hence, it is easy to find the number of retained orientations of the WO_3F_3 octahedron after this phase transition. The number of the octahedra decreases from $N_0 = 8$ to $N_1 = 4$. Such a model of ordering of WO_3F_3 is presented in Fig. 4. Thus, the transition entropy is $\Delta S_1 = R\ln(N_0/N_1) = R\ln 2$.

Upon the subsequent phase transition $I4mm \longrightarrow Cm$ at $T_2 = 414$ K, the critical order parameter has the form (η_1, η_2, 0). The process of ordering of the O and F atoms continues, and it is accompanied by the displacements of K atoms as follows: Δr(K1) = (–0.18, 0, –0.34) Å and Δr(K2) = (0.32, –0.27, – 0.13) Å. The number of the octahedron orientations decreases from $N_0 = 8$ to $N_2 = 2$. Thus, the entropy of the second

Table 3. Characteristic bond lengths in the $K_3WO_3F_3$ structure

513 K		433 K		298 K	
Bond	Length, Å	Bond	Length, Å	Bond	Length, Å
W–F	1.92(2)	W–F1	1.96(1)	W–F1	2.11(7)
		W–F2	1.91(2)	W–F2	2.00(4)
				W–F3	1.89(6)
W–O	1.87(3)	W–O1	1.88(3)	W–O1	1.74(4)
		W–O2	1.84(4)	W–O2	1.7(1)
K1–F	2.47(2)	K1–F1	2.43(1)	K1–F1	2.66(3)
		K1–F2	2.45(7)	K1–F2	2.3(1)
				K1–F3	2.02(7)
K1–O	2.83(3)	K1–O1	2.86(3)	K1–O1	2.94(5)
		K1–O2	3.02(8)	K1–O2	2.9(1)
K2–F	3.12(1)	K2–F1	3.19(3)	K2–F1	2.59(3)
		K2–F2	3.11(3)	K2–F2	3.03(8)
				K2–F3	2.4(1)
K2–O	2.65(1)	K2–O1	2.36(4)	K2–O1	2.81(7)
		K2–O2	2.55(3)	K2–O2	3.01(3)

phase transition is $\Delta S_2 = R\ln(N_1/N_2) = R\ln 2$, and the summary change in the entropy of both the phase transitions is $\Delta S_1 + \Delta S_2 = R\ln(N_0/N_2) = R\ln 4$ (Fig. 4, Table 1).

Thus-calculated changes in the entropy well agree with those measured using a DCM-2M differential scanning microcalorimeter (Table 1). A small excess of the calculated entropies of the phase transitions as compared to the measured data (Table 1) is due to the fact that the method of differential scanning gives, as a rule, underestimated values.

4. CONCLUSIONS

Thus, the structural transformations in the ferroelectric $K_3WO_3F_3$ crystal which can be schematically represented as $Fm\bar{3}m \xrightarrow[(\eta_1, 0, 0)]{11-10(\Gamma_4^-)} I4mm \xrightarrow[(\eta_1, \eta_2, 0)]{11-10(\Gamma_4^-)} Cm$. were determined using the X-ray powder diffraction in combination with the procedures of the symmetry analysis of the complete condensate of the order parameters.

ACKNOWLEDGMENTS

This study was supported by the Russian Foundation for Basic Research (project no. 09-02-00062) and the Siberian Branch of the Russian Academy of Sciences within the framework of the Interdisciplinary Project no. 34.

REFERENCES

1. I. N. Flerov, M. V. Gorev, K. S. Aleksandrov, A. Tressaud, J. Grannec, and M. Couzi, Mater. Sci. Eng., R **24** (3), 81 (1998).
2. J. Ravez, G. Peraudeau, H. Arend, S. C. Abrahams, and P. Hagenmuller, Ferroelectrics **26**, 767 (1980).
3. F. J. Brink, L. Noren, D. J. Goossens, R. L. Withers, Y. Liu, and C.-N. Xu, J. Solid State Chem. **174**, 450 (2003).
4. F. J. Brink, L. Noren, and R. L. Withers, J. Solid State Chem. **174**, 44 (2003).
5. G. von Pausewang and W. Z. Z. Rudorff, Z. Anorg. Allg. Chem. **364**, (1–2), 69 (1969).
6. V. D. Fokina, I. N. Flerov, M. V. Gorev, M. S. Molokeev, A. D. Vasiliev, and N. M. Laptash, Ferroelectrics **347**, 60 (2007).
7. I. N. Flerov, V. D. Fokina, A. F. Bovina, E. V. Bogdanov, M. S. Molokeev, A. G. Kocharova, E. I. Pogorel'tsev, and N. M. Laptash, Fiz. Tverd. Tela (St. Petersburg) **50** (3), 497 (2008) [Phys. Solid State **50** (3), 515 (2008)].
8. G. Peraudeau, J. P. Ravez, P. Hagenmuller, and H. Arend, Solid State Commun. **27**, 591 (1978).
9. V. V. Atuchin, T. A. Gavrilova, V. G. Kesler, M. S. Molokeev, and K. S. Aleksandrov, Chem. Phys. Lett. **493**, 83 (2010).
10. V. I. Mikheev, *X-Ray Determination of Minerals* (Geologiya i Okhrana Nedr, Moscow, 1957; Department of Mines and Technical Surveys, Ottawa, 1962).
11. K. S. Aleksandrov, S. V. Misyul, and E. E. Baturinets, Ferroelectrics **354**, 60 (2007).
12. H. T. Stokes, D. M. Hatch, and B. J. Campbell, *ISOTROPY: Software Package Which Applies Group Theoretical Methods to the Analysis of Phase Transitions in Crystalline Solids* (Brigham Young University, Provo, Utah, United States 2007); stokes.byu.edu/isotropy.html.
13. B. J. Campbell, H. T. Stokes, D. E. Tanner, and D. M. Hatch, J. Appl. Crystallogr. **39**, 607 (2006).
14. V. P. Sakhnenko, V. M. Talanov, and G. M. Chechin, Fiz. Met. Metalloved. **62** (5), 847 (1986).
15. O. V. Kovalev, *Irreducible and Induced Representations and Co-Representations of Fedorov's Groups* (Nauka, Moscow, 1986) [in Russian].
16. R. W. Cheary, A. A. Coelho, and J. P. Cline, J. Res. Natl. Inst. Stand. Technol. **109**, 1 (2004).
17. L. A. Solovyov, J. Appl. Crystallogr. **37**, 743 (2004).
18. E. I. Voit, A. V. Voit, A. A. Mashkovskii, N. M. Laptash, and V. Ya. Kavun, Zh. Strukt. Khim. **47** (4), 661 (2006) [J. Struct. Chem. **47** (4), 642 (2006)].
19. A. S. Krylov, Yu. V. Gerasimova, A. N. Vtyurin, V. D. Fokina, N. M. Laptash, and E. I. Voit, Fiz. Tverd. Tela (St. Petersburg) **48** (7), 1356 (2006) [Phys. Solid State **48** (7), 1356 (2006)].

Translated by Yu. Ryzhkov